Am J Clin Exp Urol 2023;11(2):136-145
www.ajceu.us /ISSN:2330-1910/AJCEU0150041

Original Article

Novel urinary tract obstruction marker discovery by multi-marker profiling of urinary extracellular vesicles derived from a rat UTO model

Nora M Haney[1*], Chi-Ju Kim[2*], Morgan D Kuczler[2], Cheng-Fan Lee[2], Kara Lombardo[1], Trinity J Bivalacqua[3], Kenneth J Pienta[2], Sarah R Amend[2]

[1]The Brady Urological Institute, Johns Hopkins School of Medicine, 600 N. Wolfe St., Baltimore, MD 21287, USA; [2]Cancer Ecology Center, The Brady Urological Institute, Johns Hopkins School of Medicine, 600 N. Wolfe St., Baltimore, MD 21287, USA; [3]Division of Urology, University of Pennsylvania Perelman School of Medicine, 3400 Civic Center Boulevard West Pavilion, Philadelphia, PA 19104, USA. [*]Equal contributors.

Received March 8, 2023; Accepted March 17, 2023; Epub April 15, 2023; Published April 30, 2023

Abstract: Introduction: Congenital urinary obstruction is a common cause of end-stage renal disease in the pediatric population. However, non-invasive diagnostics to predict which patients will benefit from early intervention are lacking. Methods: Using a rat model of upper and lower urinary tract partial obstruction and the Nanostring nCounter Fibrosis V2 Panel, we evaluated the mRNA cargo of urinary small extracellular vesicles (sEVs) and mRNA expression patterns of kidney and bladder tissues from rats with lower tract urinary obstruction and upper tract urinary obstruction. Results: While mRNA hierarchical clustering of urinary sEVs was unable to differentiate upper compared to lower tract urinary obstruction, clustering was able to detect overall disease state (UUTO or LUTO) versus healthy controls. Further, urinary sEVs carried genes unique to each treatment group (UUTO: 59 genes, LUTO: 17 genes), while only one gene was uniquely carried in the control group. Notable genes of interest found in urinary sEVs were VCAM-1 and NOS1 for UUTO, Egfr for LUTO, and Pck1 for healthy controls. Conclusion: This study provides support that differential gene expression of urinary sEV mRNA has potential to act as biomarkers in the diagnosis and prognosis of UTO. Urinary sEVs demonstrated higher numbers of unique genes representative of injury to the kidney than that of injury to the bladder. Importantly, there were genes unique to UUTO sEVs, indicating the extent and reversibility of renal damage can be independent of the function, damage, and architecture of the bladder.

Keywords: Urinary tract obstruction, urinary biomarker, extracellular vesicles

Introduction

In the pediatric population, congenital urinary obstruction is one of the most common conditions of the urinary tract and the most common cause of end stage renal disease (ESRD) [1, 2]. Urinary tract obstruction (UTO) is categorized based on location: upper tract lesions result in injury to the ipsilateral kidney and lower tract lesions place the bladder and both kidneys at risk of irreversible injury [3]. Non-invasive methods to predict which patients will benefit from early intervention are lacking. Early intervention with medication, urinary catheters, percutaneous drainage, or surgery can be performed to avoid or slow the progression to ESRD. However, intervening too early will subject the patient to unnecessary risk, and many children still progress to ESRD despite intervention [4, 5]. A reliable and non-invasive biomarker to determine the extent and reversibility of obstruction is necessary for the diagnosis, prognosis, and treatment of children with UTO.

Urinary small extracellular vesicles (sEVs) are of particular interest as a non-invasive biomarker for kidney injury and reversibility due to their high abundance and stability in biofluid [6]. sEVs contain a diversity of cargo, including proteins, nucleic acids (both RNAs and DNAs), and lipids [7-9]. In boys with posterior urethral valves (lower tract obstruction), urinary sEVs contained aquaporin-2 (AQP2), transforming growth factor-1 (TGF-β1), and L1 cell adhesion

molecule (L1CAM) proteins that correlated with estimated glomerular filtration rate [10]. In amniotic fluid-derived sEVs in patients with ureteropelvic junction (UPJ) obstruction, an upper tract obstruction, angiotensin-converting enzyme (ACE) and aminopeptidase N (AP-N) proteins were decreased [11]. mRNA sEVs cargo has been studied in other renal disease states such as glomerulosclerosis, IgA nephropathy, and diabetic nephropathy [12-14]. In lower tract obstruction, such as posterior urethral valves, the bladder is also damaged, which may confound the sEV patterns attempting to evaluate the extent of kidney disease.

No study to date has evaluated sEVs as related to obstructive bladder injury exclusively or compared differences in the patterns sEVs cargo in upper compared to lower tract urinary obstruction. Therefore, the objective of this study was to evaluate the mRNA cargo of urinary sEVs and mRNA expression patterns of kidney and bladder tissues from rats with lower UTO (bad bladder, good kidney) or upper UTO (good bladder, bad kidney).

Methods

UTO model

Male Sprague Dawley rats aged 8-10 weeks were anesthetized before performing a lower midline abdominal or left flank incision described briefly.

Upper ureteral tract obstruction (UUTO): The left ureter was exposed bluntly. Partial ureteral obstruction was induced via placement of a 0.4 mm wire next to the ureter at the UPJ and ligation of both the ureter and wire with a 6-0 nonabsorbable suture. The wire was then removed, leaving the ureter partially ligated [15]. In sham-operated rats, the ureter was identified only.

Lower urethral tract obstruction (LUTO): Partial urethral obstruction was induced by placing PE50 tubing next to the urethra at the time of surgery [16]. The urethra was identified as distal to the bladder neck and proximal to the prostate. A 6-0 nonabsorbable suture was used to ligate the bladder neck. The tubing was then removed, leaving the urethra partially obstructed at an opening of approximately 0.9 mm. In sham-operated rats, the bladder and prostate were identified alone.

Ultrasounds were obtained one week post-operatively. Bladder wall thickness and area of renal pelvis were calculated using ImageJ (NIH). At 21 days post-operatively rats were sacrificed. Bladder, kidney, urine, and serum were collected. Serum creatinine was quantified via Rat Creatinine Kit High-Performance Assays (Crystal Chem, Illinois, USA). Renal and bladder tissue were fixed in 10% buffered formalin followed by paraffin embedding for Masson's Trichrome. For RNA extraction from tissue samples, renal and bladder tissue was frozen and stored at -80°C.

RNA extraction: kidney and bladder

Frozen tissue samples were thawed. Bladder tissues (20 mg) and kidney tissue (300 mg) were ground to powder in liquid nitrogen using a mortar and pestle. The homogenized samples were processed to extract RNA using an RNeasy mini kit (Qiagen, Germany).

Urine sEV isolation and RNA extraction

Urine samples were centrifuged at 1000×g for 10 min at room temperature. The supernatant was centrifuged at 10,000×g for 20 min at 4°C. The supernatant was filtered using a 0.45 µm hydrophilic PVDF membrane syringe filter (Thermo Fisher Scientific) and stored at -80°C. Urinary sEVs were isolated using Exodisc D20 (LabSpinner, South Korea). Briefly, urine samples (≤ 1 mL) were applied to an Exodisc and processed using the bench-top operating machine (OPR-1000, LabSpinner, South Korea). Purified sEVs were retrieved using 100 µl of PBS. RNA was extracted using RNeasy micro kit (Qiagen, Germany).

Nanostring analysis

Isolated RNA was assessed with nCounter Fibrosis V2 Mouse Panel (NanoString Technologies, USA) to analyze expression of 770 mRNAs (Mouse demonstrated moderate-to-high cross-species reactivity with rat mRNA; 623 genes with > 80% identify). nCounter Low RNA Input Kit (NanoString Technologies, USA) was required to amplify sEV target genes to achieve requirements. sEV RNA was converted to cDNA and amplified using the target gene-specific primer pool with 14 cycles PCR [17, 18].

The amplified product (for sEVs) or ~100 ng of the extracted RNA (for tissue samples) was hybridized with the nCounter Panel and run on nCounter® SPRINT Profiler (NanoString Technologies, USA). Detected genes were analyzed by nSolver Analysis Software version 4.0 (NanoString Technologies, USA) and Microsoft Excel (USA).

Data was normalized in three steps. First, genes with a raw count less than the geometric means of six negative controls for each sample were marked undetected. Undetected genes for all samples in the three same groups (sEV, bladder, kidney tissue groups) were excluded for further analyses. Second, raw counts of detected genes were normalized to total counts of six spike-in positive controls (included in the panel) to calibrate sample-to-sample variations of the hybridization process. Third, the total library size of each sample for the second normalization based on the assumption of equal loading of input since the annotated housekeeping genes in the Fibrosis V2 Panel were not expected to be presented in sEV RNA samples [17].

The normalized gene counts were transformed to log2. For unsupervised hierarchical clustering analyses, normalized data was analyzed by Cluster 3.0 and Tree View [17, 19]. For visualization, log2 scaled gene counts were centered by the median of filtered genes; differentially abundant genes were represented by color spectrum from the lowest (blue) to the highest (yellow).

Gene set enrichment analysis (GSEA)

Gene Set Enrichment Analysis (GSEA) was performed using GSEA software (Broad Institute and UC San Diego) [20]. Fifty-two reference gene sets for Fibrosis V2 Panel were acquired from Nanostring and analyzed. Significantly enriched gene sets were determined by the nominal *p*-value (NOMP) < 0.05 or FDR < 0.25 cut-off.

Statistical analysis

The Tukey-Kramer posthoc test was used for pair-wise comparisons of serum creatinine, ultrasound analysis, and smooth muscle cell (SMC)/Collagen using JMP Pro 16 Statistical Software (SAS Institute, Cary, North Carolina) ($P < 0.05$). A two-tailed Student's t-test and false discovery rate (FDR, adjusted $P < 0.10$) were used to calculate the significance of the differential gene expression.

Results

Characterization of UTO

UUTO (n=5), LUTO (n=4), and control (n=4) animals were evaluated 21-days postoperatively. There was no significant difference in body mass (C: 275.4 ± 32.9 g, UUTO: 249.6 ± 26.2 g, LUTO: 258.1 ± 17.5 g). There was no significance in serum creatinine (C: 0.45 ± 0.13 mg/dL, UUTO: 0.41 ± 0.07 mg/dL, LUTO: 0.34 ± 0.08 mg/dL). Renal and bladder ultrasound one week post-operatively are shown (Supplementary Figure 1A). Quantitatively, LUTO had a significantly thicker bladder wall compared to control and UUTO ($P < 0.001$) (Supplementary Figure 1B). The area of renal pelvis was calculated, demonstrating hydronephrosis of the left kidney in UUTO compared to all other kidneys ($P < 0.001$) (Supplementary Figure 1C).

Histologic results are shown (**Figure 1A**). Trichrome demonstrates hydronephrosis in the left kidney of the UUTO group and bladder wall thickening in the LUTO samples. Quantitative analysis (**Figure 1B**, **1C**) confirmed an increased percentage of fibrosis in the left renal specimens of UUTO compared to all other kidneys ($P < 0.001$). SMC/Collagen ratios were higher in bladders of LUTO compared to control and UUTO ($P < 0.001$).

mRNA: bladder, kidney, and urinary sEVs

Across all samples, 730 of the 770 genes probed were detected. 640 genes were detected in kidney tissues, 701 genes in bladder tissues, and 510 genes in urinary sEV samples (**Figure 2A**). mRNA abundance was lower in urinary sEVs than in tissue samples, despite preamplification for sEV. Unsupervised hierarchical clustering of mRNA abundance segregated samples by tissue type (i.e., bladder vs. kidney) and sEV (**Figure 2B**).

Differential mRNA expression: kidney

Among 640 genes detected in kidneys, 567 genes were detected in UUTO, 525 genes in

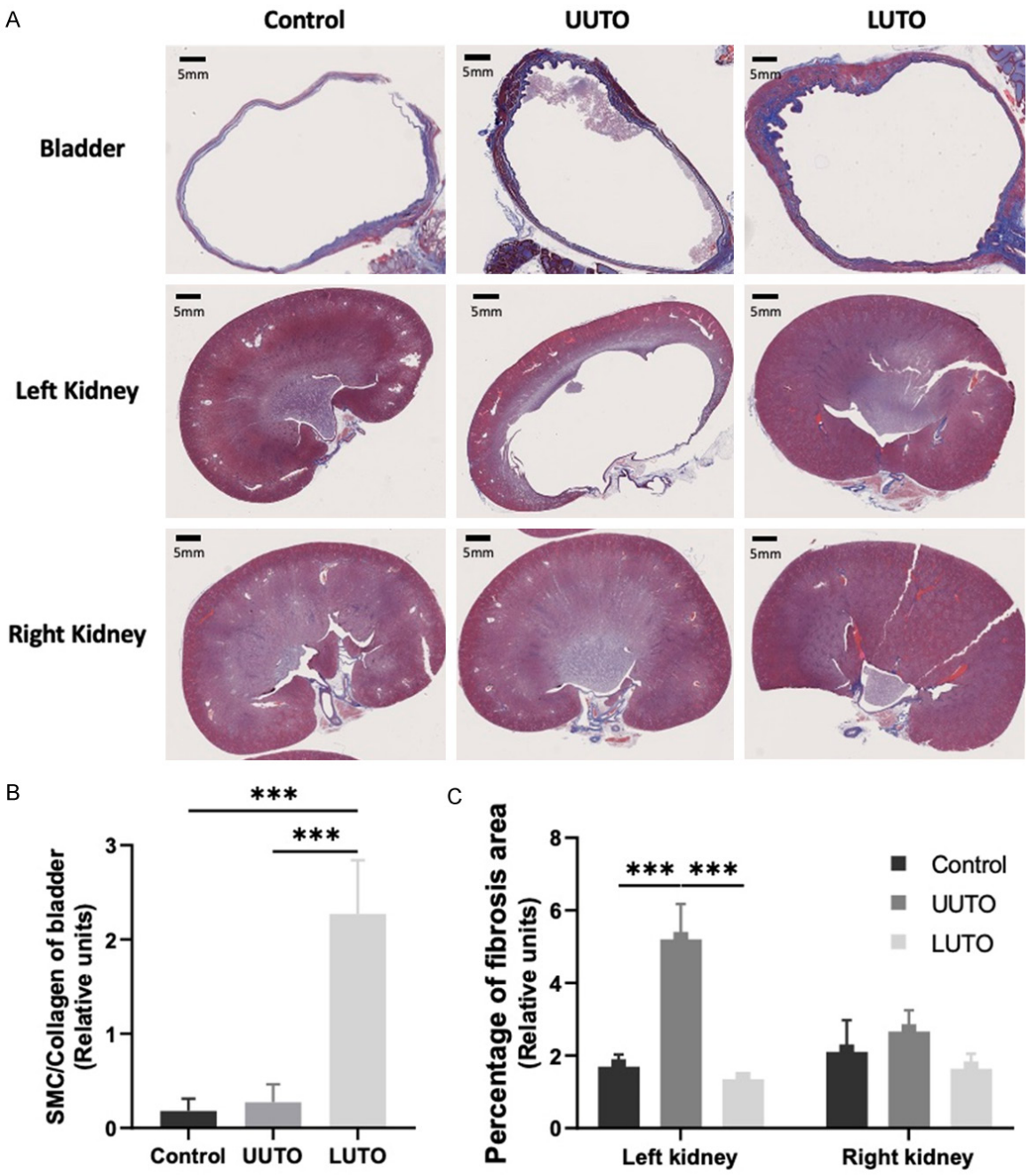

Figure 1. Histologic comparison. A. Histologic analysis using Masson's Trichrome, imaged at 0.4×, demonstrating smooth muscle hypertrophy in LUTO bladders and hydronephrosis of left kidneys in the UUTO group. B. Smooth muscle hypertrophy was present in the bladders of the LUTO groups demonstrated by SMC/Collagen ratios on trichrome analysis (C: 0.18 ± 0.13, UUTO: 0.374 ± 0.19, LUTO: 2.27 ± 0.57; $^{*}P < 0.001$ C vs. LUTO, $^{\#}P < 0.001$ UUTO vs. LUTO). C. There was a statistically significant percentage area of fibrosis (blue staining) in the left kidney of the UUTO groups on trichrome analysis (Right Kidney - C: 2.1 ± 0.88, UUTO: 2.66 ± 0.59, LUTO: 1.64 ± 0.41; Left Kidney - C: 1.7 ± 0.33, UUTO: 5.2 ± 0.98, LUTO: 1.35 ± 0.11; $^{*}P < 0.001$ Left UUTO vs. Right UUTO, $P < 0.001$ Left UUTO vs. all comparisons).

LUTO, and 589 genes in control. The mRNA expression in kidney did not cluster by group (UUTO vs. LUTO vs. Control, Supplementary Figure 2A). There was no significantly expressed gene in any comparison (FDR < 0.10, Supplementary Figure 2B-D).

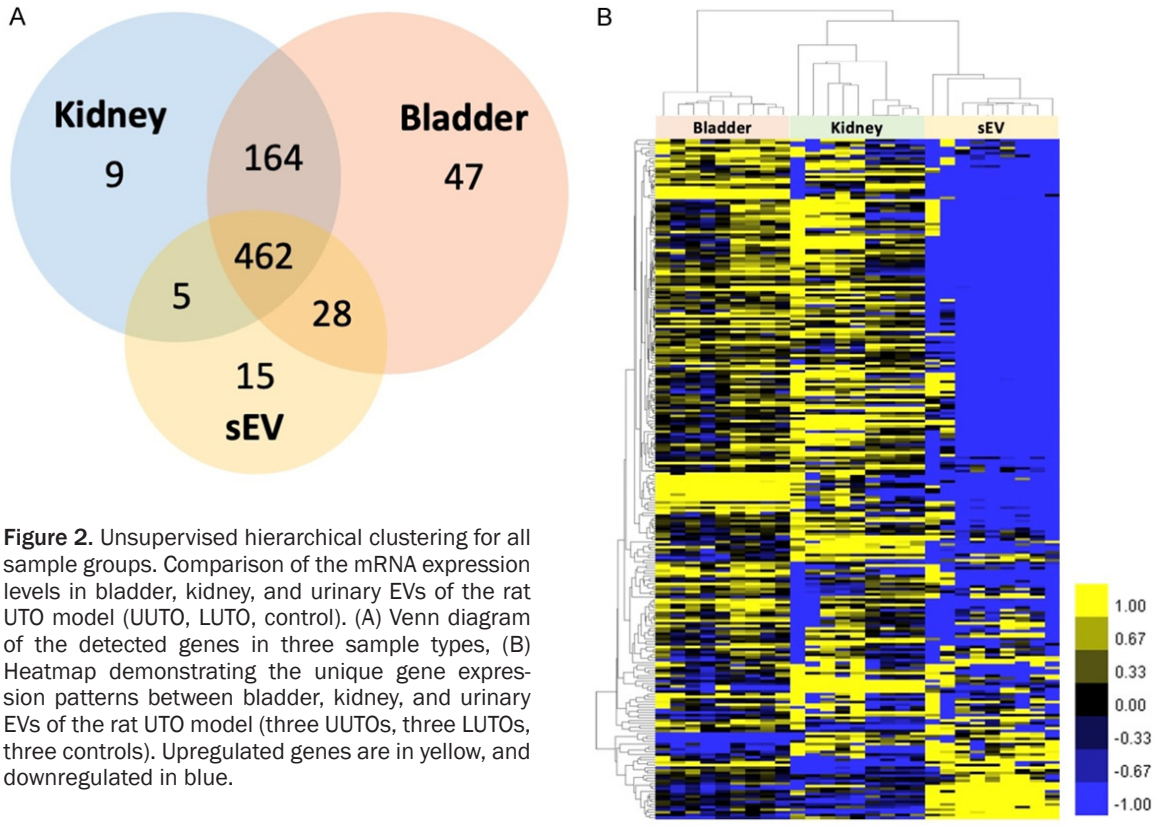

Figure 2. Unsupervised hierarchical clustering for all sample groups. Comparison of the mRNA expression levels in bladder, kidney, and urinary EVs of the rat UTO model (UUTO, LUTO, control). (A) Venn diagram of the detected genes in three sample types, (B) Heatmap demonstrating the unique gene expression patterns between bladder, kidney, and urinary EVs of the rat UTO model (three UUTOs, three LUTOs, three controls). Upregulated genes are in yellow, and downregulated in blue.

mRNA expression was further analyzed by the GSEA platform to investigate biologically relevant pathways by determining significantly (NOMP < 0.05) enriched gene sets in treatment groups. Two out of 42 tested gene sets were enriched in UUTO compared to the control: "EMT" and "ECM degradation" (Supplementary Figure 4A). Four gene sets were enriched in UUTO samples versus LUTO: "ECM synthesis", "Cytokine signaling", "ECM degradation", and "EMT" (Supplementary Figure 4B). There was no significance in UUTO versus control.

Differential mRNA expression: bladder

Among 701 mRNAs detected in bladder tissue, 575 genes were detected in UUTO, 683 in LUTO, and 631 in control. mRNA profiles in bladder did not cluster by group (Supplementary Figure 3A). Three genes were differentially expressed in UUTO bladder compared to control: *Masp1* and *Gli3* are downregulated in UUTO, while *Cfh* has increased expression (Supplementary Figure 3B). Ten genes were differentially expressed in LUTO compared to control: *Tnf* and *Gbp5* were decreased, and *Derl2*, *C8a*, *Havcr1*, *Adh4*, *Maml1*, *Anapc1*, *Prkacb*, and *H2-D1* were increased (Supplementary Figure 3C). Twenty-nine genes were differentially expressed in LUTO compared to UUTO: *Ptger4*, *Gnptab*, *Ski*, *Cdon*, *Gusb*, *Serping1*, and *Jag2* were decreased; *Irf8*, *Derl2*, *Icam1*, *Pik3r4*, *H2-Dmb2*, *Tpsb2*, *Masp1*, *Prkab2*, *Tlr1*, *Cdkn1a*, *Cyp2c29*, *Cd163*, *C8a*, *Cyp4a10/31/32*, *Adh4*, *Kng1*, *Ppard*, *Maml1*, *Ndufs5*, *Anapc1*, *Gli3*, and *Kras* were increased (Supplementary Figure 3D).

Three out of 46 GSEA gene sets were enriched in LUTO compared to control: "Proteotoxic stress", "Type II interferon", and "Type I interferon" (Supplementary Figure 5A). One gene set was enriched in UUTO compared to control: "Epigenetic modification" (Supplementary Figure 5B). Five sets were upregulated in LUTO compared to UUTO: "Senescence-associated secretory phenotype (SASP)", "PPAR signaling", "Fatty acid metabolism", "Autophagy", and "Cell cycle" (Supplementary Figure 5C).

Differential mRNA expression: urinary sEVs

Fewer unique mRNAs were detected in sEVs than in either the bladder or kidney. Among

180 mRNAs detected in sEVs, 161 were found in UUTO, 101 in LUTO, and 70 in control (**Figure 3A**). Unsupervised hierarchical clustering showed urinary sEV profiles from rats with UTO, regardless of lower or upper, cluster separately from controls (**Figure 3B**). Nineteen genes differentially enriched sEVs of UUTO compared to control: *Mtmr4, Ube2n, Furin, Got2, Ptk2, Pde2a, Cyp1a1, Sorbs1, Mob1b, Angptl4, Peli2, Tlr4, Adam9, Col4a1, Ptger4, Vcam1, Adipor1*, and *Klf5* (**Figure 3C**). Only one gene, *Wwc1*, was differentially represented in LUTO sEVs, and it was found to be depleted compared to control (**Figure 3D**). Four genes were differentially enriched in sEVs of UUTO compared to LUTO: *Sorbs1, Wwc1, App,* and *Nid1* (**Figure 3E**).

In the urinary sEV samples, 2 of 37 gene sets were upregulated in LUTO compared to control: "EMT" and "PI3K-AKT" (Supplementary Figure 6A), and one gene set was upregulated in UUTO compared to control: "ECM degradation" (Supplementary Figure 6B). One gene set was upregulated in UUTO compared to LUTO: "ECM synthesis" (Supplementary Figure 6C).

Multiple genes of urinary sEVs were uniquely present: 59 in UUTO and 17 in LUTO (**Figure 3A**; **Table 1**). Most were not co-present in kidney or bladder samples of the same group. One gene was co-present in sEV and kidney tissue in UUTO. Most listed genes were expressed in any tissue type regardless of treatment. Six genes were not expressed in any kidney tissue samples.

Discussion

Characterization confirmed successful implementation of urinary tract obstruction. In LUTO, the bladders were significantly affected by obstruction without global changes in renal function (i.e., good kidney, bad bladder). In UUTO, the left kidney was directly affected by obstruction, while serum creatinine remained normal, mimicking silent hydronephrosis seen clinically. Analysis demonstrated bladders of these groups similar to controls (i.e., bad kidney, good bladder). Histology confirmed remodeling of bladder and renal tissue with increased fibrosis in left renal specimens of UUTO and increased SMC/Collagen ratio in bladders of LUTO. The result of unsupervised hierarchical clustering for all samples differentiates three sample types correctly, indicating appropriate mRNA gene expression analysis.

In bladder samples, more genes were differentially expressed in LUTO than in UUTO, consistent with literature that LUTO alters gene expression in the bladder [21]. In a study by Ito et al, VEGF levels correlated with the thickness of detrusor muscle, whereas HIF1alpha levels increased with severity of SMC hypertrophy in response to hypoxia [21]. Notably, the number of upregulated genes in the bladder increased with time alongside SMC hypertrophy. In contrast, we found no significant gene expression in the experimental groups' kidneys compared to control. This difference found in the bladder and not the kidneys may be explained by the time-dependent response of renal tissue to obstruction. A study by Wu et al demonstrated early after obstruction, elevations in transcripts are significant and later normalize when renal damage becomes permanent [22]. While the current study is limited by a single timepoint, this time-dependent response to obstruction from the kidney compared to the bladder may support our differential gene expression results within tissue.

The sEV mRNA expression profiles were well clustered as both LUTO and UUTO clustered separately from control. While kidney and bladder mRNA profiles did not cluster, urinary sEV mRNA profiling may present potential mRNA markers in undifferentiated UTO. Yet, GSEA analysis importantly demonstrated that urinary sEVs more closely mirrored kidney injury than bladder injury. Three gene sets were significant in both kidney and sEVs: "EMT", "ECM degradation", and "ECM synthesis". In sEVs, the "EMT" set was enriched in LUTO compared to control and "ECM synthesis" was enriched in UUTO compared to LUTO. Multiple unique sets were enriched in the bladder tissue, including those related to proteotoxic stress, interferon response, and autophagy. These groupings are consistent with the literature as gene set enrichment has been shown to be time-dependent following injury in renal tissue, with early gene expression categorizing into "cellular stress" and later gene expression association with "inflammation", "collagen deposition", and "scar formation" [22].

It is well known that sEVs have limited cargo load attributed to their small size (30-200 nm) [6, 9]. Therefore, it is unsurprising that we observed fewer mRNAs as sEV cargo requiring amplification. Of the 510 distinct mRNAs

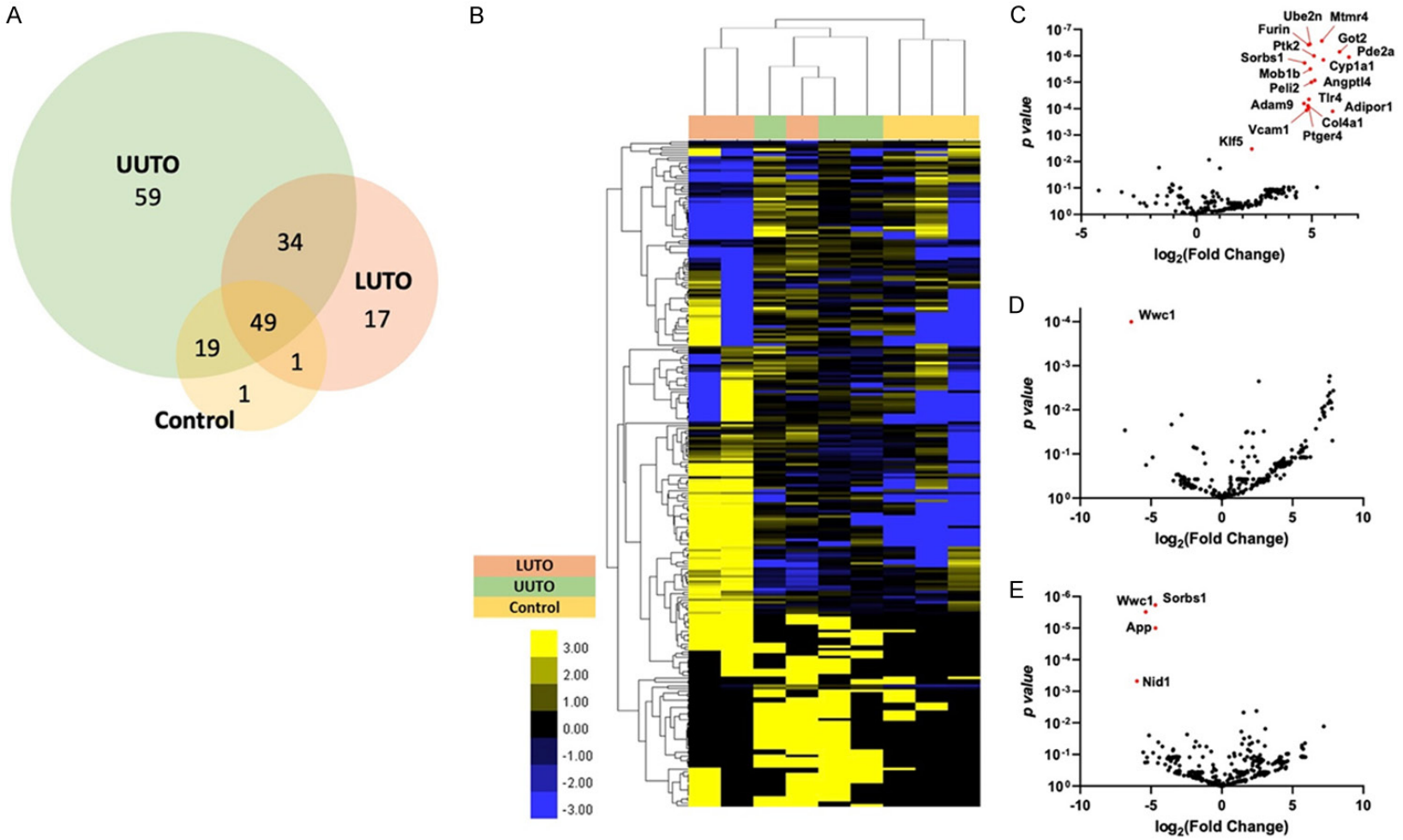

Figure 3. Differentially carried genes in urinary sEVs. Comparison of the mRNA expression levels in the urinary EVs of UUTO, LUTO, and control groups. (A) Venn diagram of the detected genes in three treatment groups with sEV samples. (B) Heatmap demonstrating the unique gene expression patterns between UUTO, LUTO, and control groups in the urinary EVs of the UTO rat model. Upregulated genes are in yellow and downregulated genes are in blue. (C) Volcano plot of the correlation between significances (*p* value) and the differential gene expression (log2 fold change) in UUTO compared to control group, (D) Volcano plot of the correlation between significances (*p* value) and the differential gene expression (log2 fold change) in LUTO compared to control group, (E) Volcano plot of the correlation between significances (*p* value) and the differential gene expression (log2 fold change) in LUTO compared to UUTO. Red dots in (C-E) indicate significant genes based on adjusted *p*-value (FDR) < 0.10.

Table 1. Uniquely presented sEV-mRNA in the disease states

Treatment groups	mRNAs
UUTO (59)	Acaa2, Adam9, Adipor1, Angptl4, App, Arhgef6, Atg101, Brpf3, [3]Ccr2, [3]Cd209e, Col4a1, Csnk2a1, Cxcl16, Cyp27a1, Dusp8, Ehmt1, [3]Eomes, Fzd2, Got2, Gpx3, [2,4]H2-Q2, Irf1, Irs1, Itgb1, Jag2, Kansl1, Kat6a, Kif3a, Lpar5, Lrp6, Maml3, Mapk1, Mmp3, Mtmr4, Mylk, Ncor2, Nid1, Nos1, Pde2a, Peli2, Pik3ca, Prf1, [3]Prkacb, Ptger4, Ptk2, Rora, Rps6kb2, Sec61b, Seh1l, Serpinf1, Sirt1, Smad2, Sorbs1, Stat3, Tgfbr2, Tlr4, [3]Tpsab1, Trrap, [1]Vcam1
LUTO (17)	Bcap31, Casp6, Egfr, Ep400, [3]Il18r1, Ilk, Klrk1, Lamtor2, Ndufb8, Pik3cb, Ppara, Sec24c, Smad6, Stat1, Stk4, Tbl1xr1, Xiap
Control (1)	Pck1

[1]Uniquely co-expressed mRNA (one gene) in all three kidney tissue samples of the same disease groups; [2]Uniquely co-expressed mRNA (one gene) among any kidney tissue samples of the same disease groups; [3]Not expressed mRNAs (six genes) in any kidney tissue samples of the same disease groups; [4]Not expressed mRNAs (one gene) in any bladder tissue samples of the same disease groups.

detected in sEVs, most were uniquely identified in either UUTO (59 genes) or LUTO (17 genes) compared to control (1 gene). These genes represent candidate sEV-derived liquid biopsy biomarkers to discriminate UUTO from LUTO and warrant future investigation and validation in clinical specimens.

One particular gene of interest identified in both urinary sEVs and all three renal specimens of UUTO was Vcam1 (vascular cell adhesion molecule 1). Involved in immune response and inflammation, levels of VCAM1 protein are elevated in urine of patients with lupus nephritis and have been associated with severity of renal insufficiency [23]. Unique to the UUTO group, NOS1 (nitric oxide synthase 1, nNOS) is part of a family that synthesizes nitric oxide from L-arginine [24]. This is relevant as studies have demonstrated the involvement of arginase (ARG) 1 and 2 isoforms and the nitric oxide pathway in UPJ obstruction and downstream renal fibrosis [24-27]. In LUTO, Egfr (epidermal growth factor receptor) involved in cell proliferation was uniquely identified. This is of interest as a LUTO-specific marker, as urinary protein levels of EGF, EGFR's ligand, was reduced in UPJ obstruction (a form of UUTO) [25]. Further, the SHH (sonic hedgehog) signaling pathway, involved in neurite formation and SMC apoptosis in bladder injury, is known to cross-talk with the EGF pathway [28, 29]. In the control, Pck1 (phosphoenolpyruvate carboxykinase 1) was expressed in urinary sEVs, which could be an indicator of an overall healthy state. This gene, highly expressed in the kidney, is a control point for gluconeogenesis regulation; deficiencies in this gene are associated with growth failure and inborn errors of metabolism [30]. Importantly, most genes uniquely detected in urinary sEVs were expressed in any tissue type regardless of treatment type. Thus, urinary sEVs may present a novel method of detecting specific upper vs. lower tract obstruction unable to be gleaned from tissue itself.

Although this study demonstrated promise that urinary sEVs might provide molecular signatures of UTO, there are limitations. We anticipated that distinct gene expression profiles in kidney and bladder tissues would differentiate the experimental groups and control. Unexpectedly, unsupervised hierarchical clustering of mRNA expression did not differentiate between treatment groups in either kidney or bladder. This raises the possibility that the severity of partial UTO rat model and timeline utilized were not suitable to change the overall gene expression patterns at a tissue level or that overall gene signatures are more significantly deranged closer to the time of injury (i.e., day three after operation). Notably, we did detect unique differences in sEV mRNA cargo between treatment groups (UUTO vs. LUTO and experimental groups vs. control), highlighting the promise of sEV biomarkers. Future studies will discern if the tissue-derived gene expression patterns compared to the urinary sEV specimens are due to time-dependent response or possibly rate of adaptation to the injury.

In this study, urinary sEVs demonstrated higher numbers of unique genes representative of injury to the kidney than injury to the bladder. This provides support that urinary sEVs potential to prognosticate UUTO extent and reversibil-

ity of renal damage can be independent of the function, damage, and architecture of the bladder. Yet, given the inability to differentiate the type of obstruction (upper vs. lower) using clustering techniques of urinary sEVs, the authors emphasize the need to be cognizant of simultaneous damage to the bladder when evaluating prognostic biomarkers for ESRD. These findings advocate that urinary sEVs remain a promising non-invasive material to diagnose UTO but highlights the extent of the knowledge gap needed to be bridged before bringing this biomarker to the clinical setting.

Acknowledgements

Kim CJ was supported by the Basic Science Research Program through the National Research Foundation of Korea funded by the Ministry of Education (2021R1A6A3A140-43146), and the Smart Healthcare Research Center at UNIST. Pienta KJ was supported by National Cancer Institute grants U54CA1438-03, CA163124, CA093900, and CA143055, and the Prostate Cancer Foundation. Amend SR was supported by the US Department of Defense CDMRP/PCRP 367 (W81XWH-20-10353), the Patrick C Walsh Prostate Cancer Research Fund, and the Prostate Cancer Foundation.

Disclosure of conflict of interest

K.J.P. is a consultant for CUE Biopharma, Inc., and holds equity interest in CUE Biopharma, Inc., Keystone Biopharma, Inc., and PEEL Therapeutics, Inc. SRA holds equity interest in Keystone Biopharma, Inc.

Address correspondence to: Nora M Haney, The Brady Urological Institute, Johns Hopkins School of Medicine, 600 N. Wolfe St., Baltimore, MD 21287, USA. E-mail: nhaney2@jhmi.edu

References

[1] Chevalier RL. Congenital urinary tract obstruction: the long view. Adv Chronic Kidney Dis 2015; 22: 312-9.

[2] Sanderson KR, Yu Y, Dai H, Willig LK and Warady BA. Outcomes of infants receiving chronic peritoneal dialysis: an analysis of the USRDS registry. Pediatr Nephrol 2019; 34: 155-162.

[3] Ingraham SE and McHugh KM. Current perspectives on congenital obstructive nephropathy. Pediatr Nephrol 2011; 26: 1453-61.

[4] Bilgutay AN, Roth DR, Gonzales ET Jr, Janzen N, Zhang W, Koh CJ, Gargollo P and Seth A. Posterior urethral valves: risk factors for progression to renal failure. J Pediatr Urol 2016; 12: 179, e1-7.

[5] Coquillette M, Lee RS, Pagni SE, Cataltepe S and Stein DR. Renal outcomes of neonates with early presentation of posterior urethral valves: a 10-year single center experience. J Perinatol 2020; 40: 112-117.

[6] Li X and Yang L. Urinary exosomes: emerging therapy delivery tools and biomarkers for urinary system diseases. Biomed Pharmacother 2022; 150: 113055.

[7] Merchant ML, Rood IM, Deegens JKJ and Klein JB. Isolation and characterization of urinary extracellular vesicles: implications for biomarker discovery. Nat Rev Nephrol 2017; 13: 731-749.

[8] Buzás EI, Tóth EÁ, Sódar BW and Szabó-Taylor KÉ. Molecular interactions at the surface of extracellular vesicles. Semin Immunopathol 2018. 40: 453-464.

[9] Cricrì G, Bellucci L, Montini G and Collino F. Urinary extracellular vesicles: uncovering the basis of the pathological processes in kidney-related diseases. Int J Mol Sci 2021; 22: 6507.

[10] Trnka P, Ivanova L, Hiatt MJ and Matsell DG. Urinary biomarkers in obstructive nephropathy. Clin J Am Soc Nephrol 2012; 7: 1567-75.

[11] Liu R, Zhang W, Luo M, Qin X, Yang F and Wei Q. iTRAQ-based proteomics and in vitro experiments reveals essential roles of ACE and AP-N in the renin-angiotensin system-mediated congenital ureteropelvic junction obstruction. Exp Cell Res 2020; 393: 112086.

[12] Lv LL, Cao YH, Pan MM, Liu H, Tang RN, Ma KL, Chen PS and Liu BC. CD2AP mRNA in urinary exosome as biomarker of kidney disease. Clin Chim Acta 2014; 428: 26-31.

[13] Abe H, Sakurai A, Ono H, Hayashi S, Yoshimoto S, Ochi A, Ueda S, Nishimura K, Shibata E, Tamaki M, Kishi F, Kishi S, Murakami T, Nagai K and Doi T. Urinary exosomal mRNA of WT1 as diagnostic and prognostic biomarker for diabetic nephropathy. J Med Invest 2018; 65: 208-215.

[14] Feng Y, Lv LL, Wu WJ, Li ZL, Chen J, Ni HF, Zhou LT, Tang TT, Wang FM, Wang B, Chen PS, Crowley SD and Liu BC. Urinary exosomes and exosomal CCL2 mRNA as biomarkers of active histologic injury in IgA nephropathy. Am J Pathol 2018; 188: 2542-2552.

[15] Thornhill BA and Chevalier RL. Chevalier, variable partial unilateral ureteral obstruction and its release in the neonatal and adult mouse. Methods Mol Biol 2012; 886: 381-92.

[16] Tassone NM, Li B, Devine MY, Hausner PM, Patel MS, Gould AD, Kochan KS, Dettman RW and Gong EM. Voided volumes predict degree

of partial bladder outlet obstruction in a murine model. Am J Clin Exp Urol 2018; 6: 189-196.
[17] Dong L, Huang CY, Johnson EJ, Yang L, Zieren RC, Horie K, Kim CJ, Warren S, Amend SR, Xue W and Pienta KJ. High-throughput simultaneous mRNA profiling using nCounter technology demonstrates that extracellular vesicles contain different mRNA transcripts than their parental prostate cancer cells. Anal Chem 2021; 93: 3717-3725.
[18] Kuczler MD, Zieren RC, Dong L, de Reijke TM, Pienta KJ and Amend SR. Advancements in the identification of EV derived mRNA biomarkers for liquid biopsy of clear cell renal cell carcinomas. Urology 2022; 160: 87-93.
[19] Eisen MB, Spellman PT, Brown PO and Botstein D. Cluster analysis and display of genome-wide expression patterns. Proc Natl Acad Sci U S A 1998; 95: 14863-14868.
[20] Subramanian A, Tamayo P, Mootha VK, Mukherjee S, Ebert BL, Gillette MA, Paulovich A, Pomeroy SL, Golub TR, Lander ES and Mesirov JP. Gene set enrichment analysis: a knowledge-based approach for interpreting genome-wide expression profiles. Proc Natl Acad Sci U S A 2005; 102: 15545-15550.
[21] Ito S, Nomura T, Ueda T, Inui S, Morioka Y, Honjo H, Fukui A, Fujihara A, Hongo F and Ukimura O. Gene expression profiles during tissue remodeling following bladder outlet obstruction. Sci Rep 2021; 11: 13171.
[22] Wu B, Gong X, Kennedy WA and Brooks JD. Identification of transcripts associated with renal damage due to ureteral obstruction as candidate urinary biomarkers. Am J Physiol Renal Physiol 2018; 315: F16-F26.
[23] Khamchun S, Thammakhan N and Lomthong P. Systematic evaluation of urinary VCAM1 as novel biomarker for prognosis of lupus nephritis. Clin Lab 2021; 67.
[24] Miyajima A, Chen J, Poppas DP, Vaughan ED Jr and Felsen D. Role of nitric oxide in renal tubular apoptosis of unilateral ureteral obstruction. Kidney Int 2001; 59: 1290-303.
[25] Lacroix C, Caubet C, Gonzalez-de-Peredo A, Breuil B, Bouyssié D, Stella A, Garrigues L, Le Gall C, Raevel A, Massoubre A, Klein J, Decramer S, Sabourdy F, Bandin F, Burlet-Schiltz O, Monsarrat B, Schanstra JP and Bascands JL. Label-free quantitative urinary proteomics identifies the arginase pathway as a new player in congenital obstructive nephropathy. Mol Cell Proteomics 2014; 13: 3421-34.
[26] Manucha W and Vallés PG. Cytoprotective role of nitric oxide associated with Hsp70 expression in neonatal obstructive nephropathy. Nitric Oxide 2008; 18: 204-15.
[27] Yamaleyeva LM, Lindsey SH, Varagic J, Zhang LL, Gallagher PE, Chen AF and Chappell MC. Amelioration of renal injury and oxidative stress by the nNOS inhibitor L-VNIO in the salt-sensitive mRen2.Lewis congenic rat. J Cardiovasc Pharmacol 2012; 59: 529-38.
[28] Fröhlich H, Bahamondez G, Götschel F and Korf U. Dynamic bayesian network modeling of the interplay between EGFR and hedgehog signaling. PLoS One 2015; 10: e0142646.
[29] Zhang H, Xu S, He D, Wang X and Zhu G. Spatiotemporal expression of SHH/GLI signaling in human fetal bladder development. Front Pediatr 2021; 9: 765255.
[30] Oishi K, Siegel C, Cork EE, Chen H and Imagawa E. Novel missense variants in PCK1 gene cause cytosolic PEPCK deficiency with growth failure from inadequate caloric intake. J Hum Genet 2021; 66: 321-325.

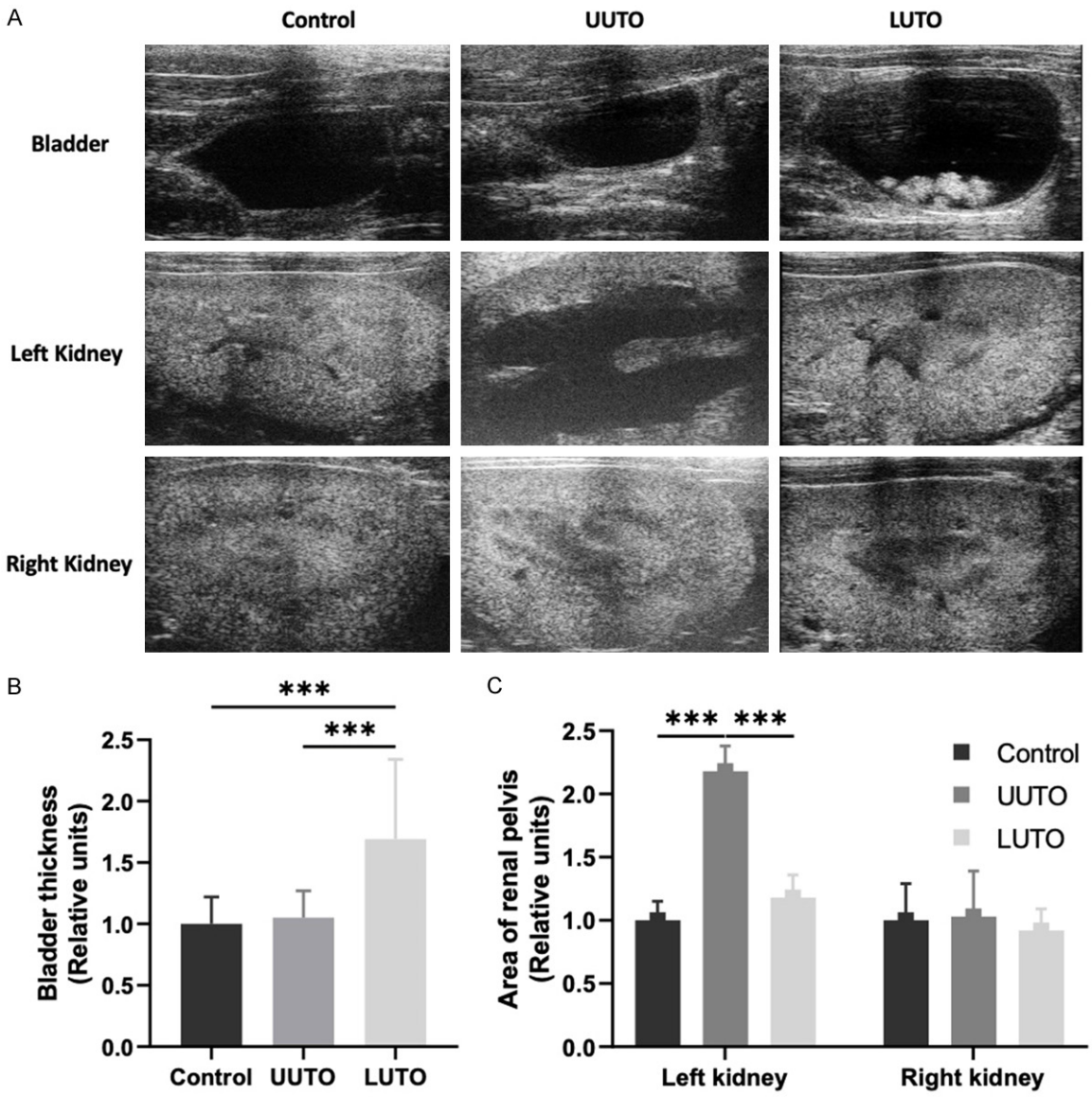

Supplementary Figure 1. Ultrasonagraphic comparison. A. Renal bladder ultrasound images at 1 week post-operatively. Compared to control, the left renal pelvis is grossly hydronephrotic compared to all other kidneys. The LUTO group demonstrates bladder wall thickening and echogenic bladder calculi compared to control and UUTO groups. B. The bladder wall of the LUTO group was statistically significantly thicker than those of control and UUTO groups (C: 1.00 ± 0.22 relative units, UUTO: 1.05 ± 0.22 relative units, LUTO: 1.69 ± 0.65 relative units; $^{*}P < 0.001$ control vs. LUTO, $^{\#}P < 0.001$ UUTO vs. LUTO). C. The left kidney of the UUTO group was hydronephrotic compared to its contralateral kidney and all other kidneys of other groups (Right Kidney - control: 1.00 ± 0.19, UUTO: 1.03 ± 0.36, LUTO: 0.92 ± 0.17; Left Kidney - control: 1.00 ± 0.15, UUTO: 2.18 ± 0.20, LUTO: 1.18 ± 0.18; $^{*}P < 0.001$ Left UUTO vs. Right UUTO, $^{\#}P < 0.001$ Left UUTO vs. all comparisons).

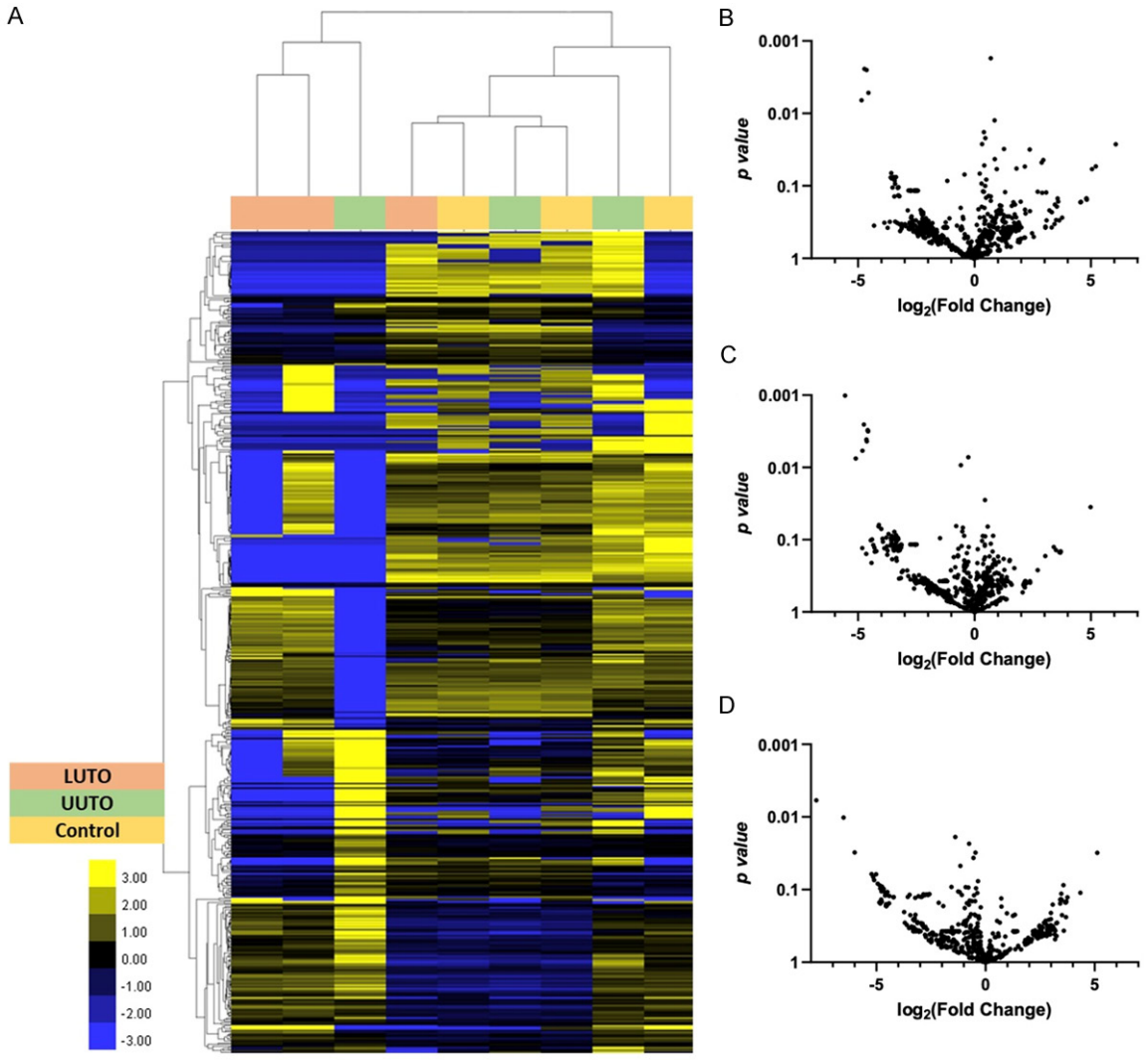

Supplementary Figure 2. Differential gene expression in Kidney. Comparison of the mRNA expression levels in the kidney of UUTO, LUTO, and control groups. A. Heatmap demonstrating the unique gene expression patterns between UUTO, LUTO, and control groups in the kidney of the UTO rat model. Upregulated genes are in yellow, and downregulated in blue. B. Volcano plot of the correlation between significances (*p* value) and the differential gene expression (log2 fold change) in UUTO compared to control group. C. Volcano plot of the correlation between significances (*p* value) and the differential gene expression (log2 fold change) in LUTO compared to control group. D. Volcano plot of the correlation between significances (*p* value) and the differential gene expression (log2 fold change) in LUTO compared to UUTO.

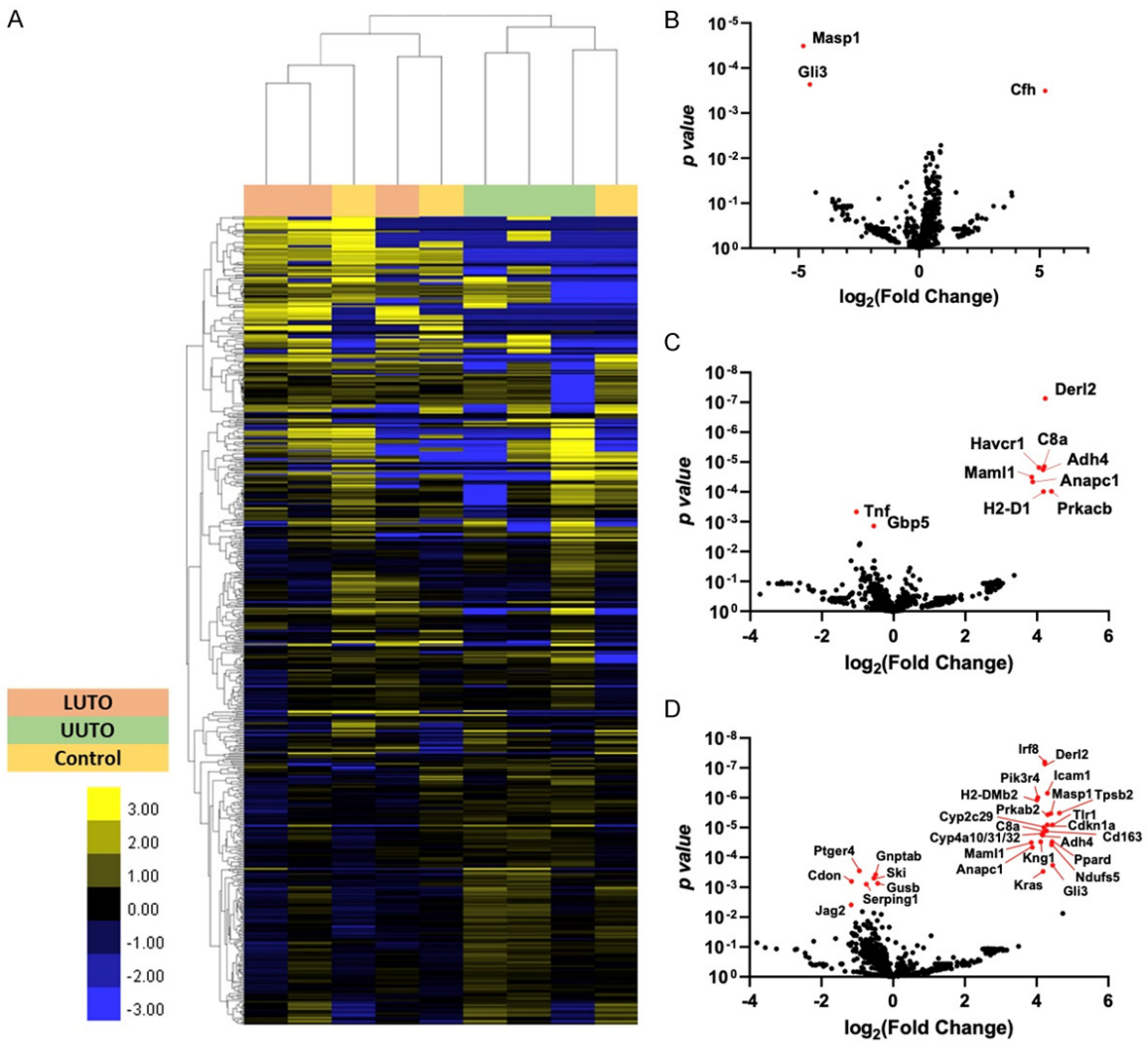

Supplementary Figure 3. Differential gene expression in Bladder. Comparison of the mRNA expression levels in the bladder of UUTO, LUTO, and control groups. (A) Heatmap demonstrating the unique gene expression patterns between UUTO, LUTO, and control groups in the bladder of the UTO rat model. Upregulated genes are in yellow and downregulated in blue. (B) Volcano plot of the correlation between significances (*p* value) and the differential gene expression (log2 fold change) in UUTO compared to control group, (C) Volcano plot of the correlation between significances (*p* value) and the differential gene expression (log2 fold change) in LUTO compared to control group, (D) Volcano plot of the correlation between significances (*p* value) and the differential gene expression (log2 fold change) in LUTO compared to UUTO. Red dots in (C, D) indicate significant genes based on adjusted *p*-value (FDR) < 0.10.

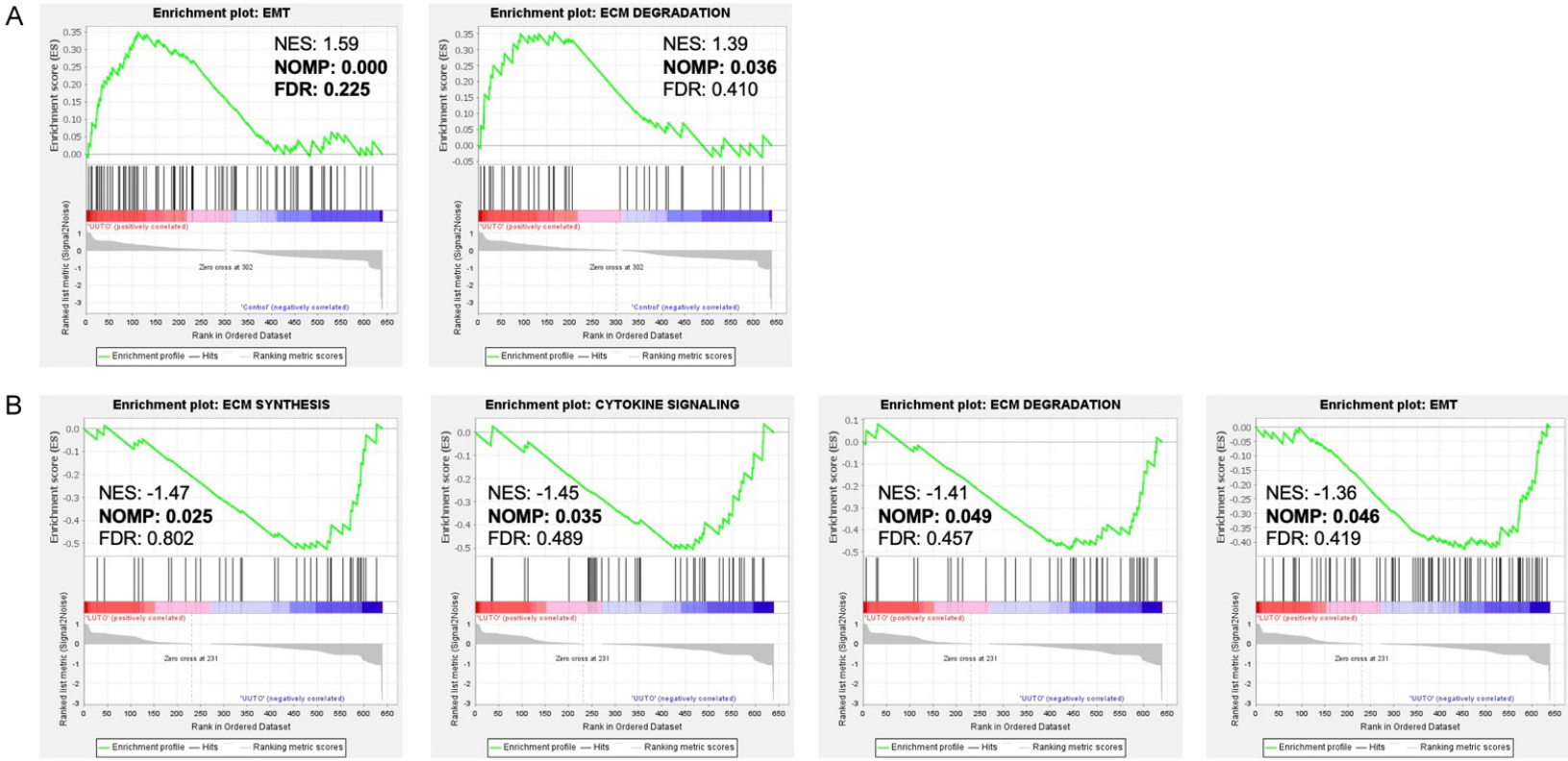

Supplementary Figure 4. Gene set enrichment analysis (GSEA) of kidney samples. Enrichment plots of significantly enriched gene sets in (A) the UUTO group versus the control group, (B) the LUTO group versus the UUTO group. Statistically significance is determined by nominal *p* value (NOMP) below 0.05. NES: normalized enrichment score, FDR: false discovery rate.

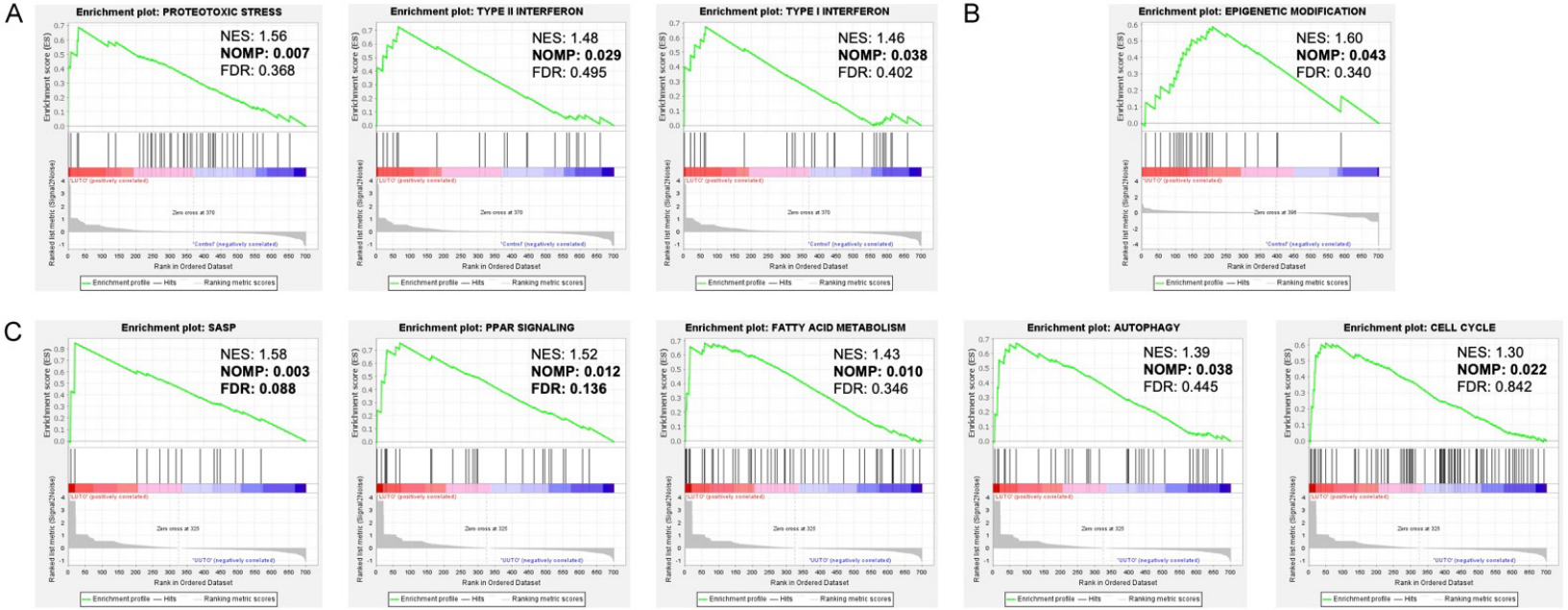

Supplementary Figure 5. Gene set enrichment analysis (GSEA) of bladder samples. Enrichment plots of significantly enriched gene sets in (A) the LUTO group versus the control group, (B) the UUTO group versus the control group, (C) the LUTO group versus the UUTO group. Statistically significance is determined by nominal *p* value (NOMP) below 0.05. NES: normalized enrichment score, FDR: false discovery rate.

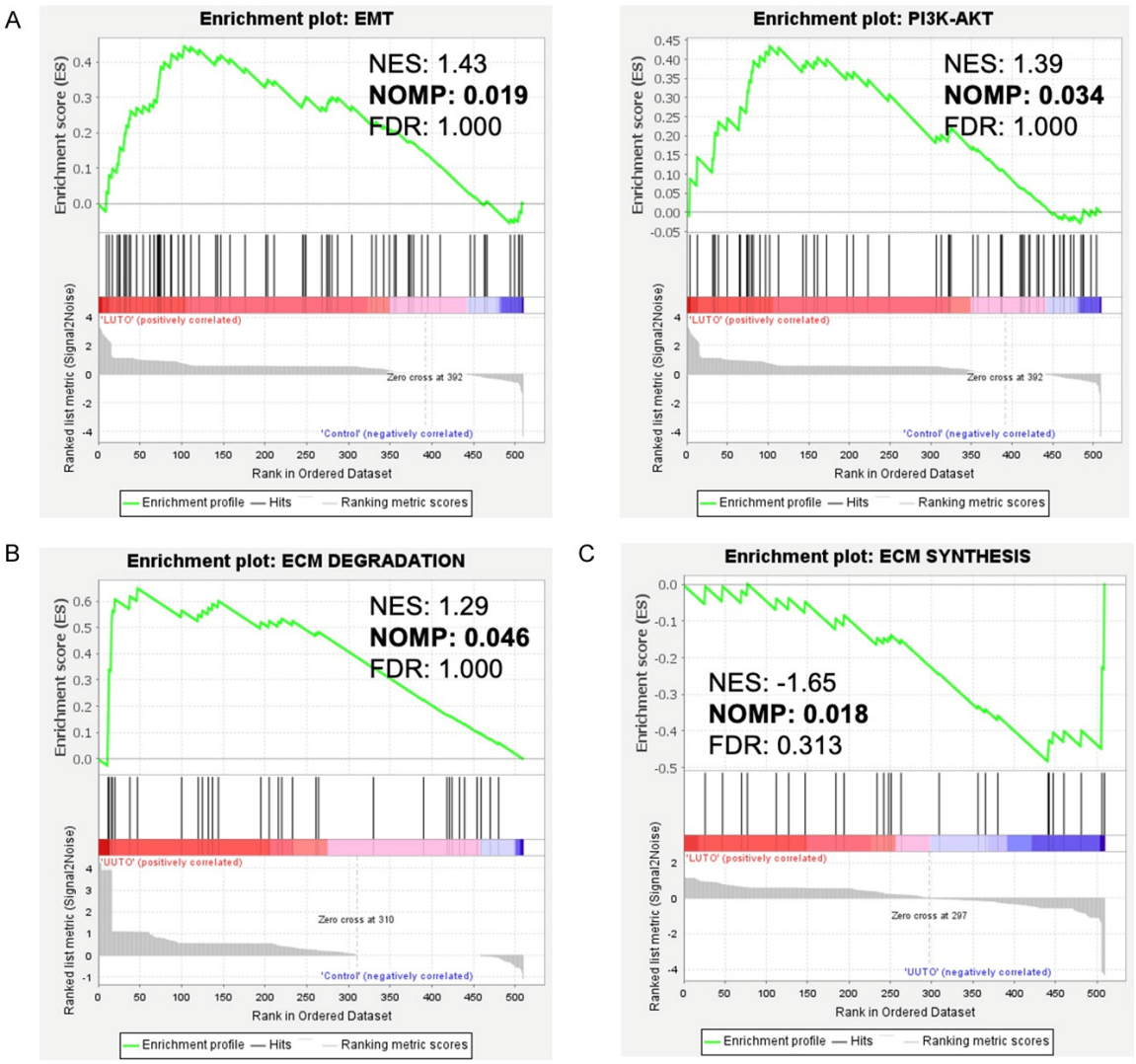

Supplementary Figure 6. Gene set enrichment analysis (GSEA) of EV samples. Enrichment plots of significantly enriched gene sets in (A) the LUTO group versus the control group, (B) the UUTO group versus the control group, (C) the LUTO group versus the UUTO group. Statistically significance is determined by nominal *p* value (NOMP) below 0.05. NES: normalized enrichment score, FDR: false discovery rate.